HHS Public Access

Author manuscript

*Biosens Bioelectron*. Author manuscript; available in PMC 2016 July 15.

Published in final edited form as:

*Biosens Bioelectron*. 2016 July 15; 81: 8–14. doi:10.1016/j.bios.2016.01.073.

# Sensitive DNA detection and SNP discrimination using ultrabright SERS nanorattles and magnetic beads for malaria diagnostics

**Hoan T. Ngo**[a,b], **Naveen Gandra**[a,b], **Andrew M. Fales**[a,b], **Steve M. Taylor**[a,c], and **Tuan Vo-Dinh**[a,b,d,*]

[a]Fitzpatrick Institute for Photonics, Duke University, Durham, NC 27708, USA

[b]Department of Biomedical Engineering, Duke University, Durham, NC 27708, USA

[c]Department of Medicine & Duke Global Health Institute, Duke University, Durham, NC 27708, USA

[d]Department of Chemistry, Duke University, Durham, NC 27708, USA

## Abstract

One of the major obstacles to implement nucleic acid-based molecular diagnostics at the point-of-care (POC) and in resource-limited settings is the lack of sensitive and practical DNA detection methods that can be seamlessly integrated into portable platforms. Herein we present a sensitive yet simple DNA detection method using a surface-enhanced Raman scattering (SERS) nanoplatform: the ultrabright SERS nanorattle. The method, referred to as the nanorattle-based method, involves sandwich hybridization of magnetic beads that are loaded with capture probes, target sequences, and ultrabright SERS nanorattles that are loaded with reporter probes. Upon hybridization, a magnet was applied to concentrate the hybridization sandwiches at a detection spot for SERS measurements. The ultrabright SERS nanorattles, composed of a core and a shell with resonance Raman reporters loaded in the gap space between the core and the shell, serve as SERS tags for signal detection. Using this method, a specific DNA sequence of the malaria parasite *Plasmodium falciparum* could be detected with a detection limit of approximately 100 attomoles. Single nucleotide polymorphism (SNP) discrimination of wild type malaria DNA and mutant malaria DNA, which confers resistance to artemisinin drugs, was also demonstrated. These test models demonstrate the molecular diagnostic potential of the nanorattle-based method to both detect and genotype infectious pathogens. Furthermore, the method's simplicity makes it a suitable candidate for integration into portable platforms for POC and in resource-limited settings applications.

*Corresponding author at: Department of Biomedical Engineering, Duke University, Durham, NC 27708, USA. tuan.vodinh@duke.edu (T. Vo-Dinh).

**Notes**

Material and methods can be found in the Supplementary material.

**Conflict of interest**

The authors declare no conflict of interest.

**Keywords**

Surface-enhanced Raman Scattering; Nanoparticle; DNA Detection; SNP discrimination; Molecular diagnostics; Point-of-care; Biosensing

## 1. Introduction

Molecular diagnostics is of paramount importance in medicine, biosensing, forensic science, etc. with many advantages such as high specificity, high sensitivity, serotyping capability, and mutation detection. Currently, the gold standard of nucleic acid-based molecular diagnostics tests involves polymerase chain reaction (PCR). PCR is highly sensitive with a single to few copies of target detection limit. However, it requires relatively bulky, expensive equipment, skilled workers, and is quite labor-intensive and time-consuming (Niemz et al., 2011). Until recently, PCR tests have mainly been conducted in laboratories or hospitals. Development of rapid, easy-to-use, cost-effective, high accuracy DNA tests for molecular diagnostics at the POC and in resource-limited settings is highly needed. Such techniques will be helpful not only in developing countries but also in developed countries.

Many efforts have been devoted to develop new DNA detection methods for molecular diagnostics at the POC. Since the copy number of target DNA sequences is usually low, most of the existing methods utilize (1) target amplification or/and (2) signal amplification to achieve sufficient sensitivity. In target amplification methods (e.g. PCR, loop-mediated isothermal amplification, etc.), target sequences are amplified many million-fold using enzymatic reactions. Target amplification methods, therefore, are very sensitive. However, due to high level of amplification, trace amounts of contaminants could serve as templates and be amplified, making these methods susceptible to false positives. In addition, the presence of inhibitors can prevent enzymatic amplification, thus target purification is often required (Bessetti, 2007). Finally, the inherent biases in enzymatic amplifications may prevent accurate quantification (Mayr et al., 2016).

As an alternative to target amplification, signal amplification methods can mitigate these risks, but require strong signal amplification. One method of signal amplification is SERS (Lane et al., 2015; Schlücker, 2014), a phenomenon in which Raman scattering of molecules adsorbed on metallic nanostructures is enhanced many million-fold. SERS has been reported as a sensitive analytical technique, as demonstrated by its ability to detect single molecules (Darby et al., 2014; Kneipp et al., 1997; Nie and Emery, 1997). Based on SERS, our laboratory has developed different chemical and biological sensing methods for medical diagnostics and environmental monitoring (Vo-Dinh, 1998; Vo-Dinh et al., 2010; Vo-Dinh et al., 2013; Vo-Dinh et al., 2015). Compared to fluorescence, SERS has several advantages, including being more stable against photobleaching due to the extremely short lifetimes of Raman scattering (Doering and Nie, 2003). A SERS spectral peak is two orders of magnitude narrower than a fluorescence peak, making SERS more suitable for multiplex detection. With the same fluorophores, surface-enhanced resonance Raman scattering (SERRS) detection limit has been shown to be three orders of magnitude lower than of fluorescence (Faulds et al., 2004).

SERS-based DNA detection has been investigated widely (Cao et al., 2002; Fabris et al., 2007; Faulds et al., 2008; Gao et al., 2013; He et al., 2011; Hu et al., 2010; Kang et al., 2010; Li et al., 2012; Li et al., 2013b; Ngo et al., 2014a; Ngo et al., 2014b; Ngo et al., 2013, 2015; Qi et al., 2014; Sun et al., 2007; Xu et al., 2015). The Mirkin group developed gold nanoparticle probes labeled with oligonucleotides and Raman-active dyes for multiplex detection of DNA (Cao et al., 2002) with an unoptimized detection limit of 20 fM. Hu et al. utilized multilayer metal-molecule-metal nanojunctions to detect HIV-1 DNA at a sub-aM limit with single base mismatch discrimination (Hu et al., 2010). He et al. developed silicon nanowires coated with in situ grown silver nanoparticles for DNA detection at a 1 fM limit (He et al., 2011). Li et al. used a plasmonic nanorice and triangle nanoarray for detection of Hepatitis B virus DNA at a 50 aM limit (Li et al., 2013b). Although sensitive, integrating these methods into portable platforms for POC applications is still a challenge.

Herein, we developed a sensitive SERS-based DNA detection method, referred to as the nanorattle-based method, that is suitable for integrating into lab-on-chip systems for POC molecular diagnostics. The method employs sandwich hybridization of magnetic beads that are loaded with capture probes, target sequences, and ultrabright SERS nanorattles that are loaded with reporter probes. The nanorattles are used as SERS tags. Upon hybridization, sandwiches of magnetic bead–target–nanorattle were formed, and then a magnet was applied to concentrate the hybridization sandwiches at a detection spot for SERS measurements. Although the use of sandwich hybridization of magnetic bead, target sequence, and SERS tag for DNA detection has been reported previously (Donnelly et al., 2014; Li et al., 2013a; Xu et al., 2012; Zhang et al., 2011), the novelty of our method lies in the use of the nanorattle. The rationale behind this is to improve the sensitivity by using a much brighter SERS tag. Most previously-used SERS tags are composed of a nanoparticle (gold or silver) coated with Raman reporters and DNA probes on its surface; in these structures, SERS tag brightness is limited by the presence of only a submonolayer of Raman reporters on the nanoparticle’s surface. In contrast, our ultrabright SERS nanorattle has a core-gap-shell structure with Raman reporters trapped in the gap between the nanorattle’s core and shell. The gap is on the nanometer scale, providing room for a large number of Raman reporters. In addition, the nanosize gap between the core and the shell possesses an intense electromagnetic field (E field) enhancement, further improving the nanorattle’s SERS brightness. Compared to Raman reporter-labeled gold nanospheres, our ultrabright SERS nanorattles are approximately three orders of magnitude brighter. Furthermore, SERS signal stability is also improved. The nanorattle has Raman reporters encapsulated by a complete metallic shell, which can prevent SERS signal degradation due to reporter desorption.

Malaria is a global health threat to children and adults in tropical regions. Ninety-seven countries suffer ongoing transmission of malaria parasites, which imperil 3.4 billion people annually. In 2013, malaria caused an estimated 207 million infection cases and over 600,000 deaths (WHO, 2014). Mutant strains of the malaria parasite *Plasmodium falciparum* that are resistant to artemisinin drugs (Art-R), a first-line therapy for malaria, have been reported (Dondorp et al., 2009; Noedl et al., 2008). It is important to develop new malaria diagnostics methods that can be used at the POC and are able to identify mutant malaria parasites. Using the nanorattle-based method, we demonstrate that a specific DNA sequence of the malaria parasite *P. falciparum* can be detected with approximately 100-attomole detection limit.

Furthermore, the SNP discrimination between wild type and mutant malaria parasite DNA sequence, which confers resistance to Art-R, is also demonstrated. The use of magnetic beads and the method's simplicity make it a suitable candidate for automation and integration into lab-on-chip systems for POC molecular diagnostics.

## 2. Results and discussion

### 2.1. Detection scheme

The detection scheme of the nanorattle-based method is shown in Fig. 1. Magnetic beads and nanorattles are functionalized with DNA capture probes and DNA reporter probes, respectively. The two probes are designed to be complementary to the two ends of the target sequences. Detection is conducted by subsequently adding to sample solutions of interest magnetic beads that are loaded with capture probes and nanorattles that are loaded with reporter probes. In the presence of the target sequences, hybridization sandwiches of magnetic bead-target sequence-nanorattle are formed (Fig. 1a). A permanent magnet is used to concentrate the magnetic bead-target sequence-nanorattle sandwiches onto a small spot for SERS measurement (Fig. 1b).

### 2.2. Nanorattle

The SERS nanorattle synthesis process is shown in Fig. 2a. AuNP were first synthesized followed by Ag coating to form Au–Ag core–shell structures (AuNP@Ag). Galvanic replacement (Xia et al., 2013) was then used to turn the Ag shells into porous Au–Ag cages containing AuNP inside (AuNP@Cage). Raman reporters were then loaded into the AuNP@Cage with the assistance of a phase-change material (Moon et al., 2011). The porous cages were then turned into complete shells by a final Au coating to form SERS nanorattles. TEM images of the synthesized SERS nanorattles are shown in Fig. 2b. The average particle size is approximately 60 nm. The core-gap-shell structure is clearly observable. It is noteworthy that several different core-gap-shell structures have been previously reported (Chen et al., 2006; Khalavka et al., 2009; Sun et al., 2004). In our work, by loading HITC Raman reporters into the gap space between the core and the shell, SERS-encoded nanorattles were obtained.

SERS measurements showed that SERS nanorattles exhibit intense SERS signal, more than three orders of magnitude stronger than gold nanospheres coated with the same Raman reporters (Fig. S1). We attribute the nanorattle's intense SERS brightness to two factors. First, with a nanosize gap space between the nanorattle's core and shell, the nanorattle could be loaded with a higher number of Raman reporters in comparison with number of reporters in a monolayer coating on a gold nanosphere's surface. Second, the E field enhancement in the gap space of the nanorattle was estimated to be several times higher than the enhancement on gold nanosphere's surface. Since SERS enhancement strongly depends on E field enhancement with a fourth power dependence (Schatz and Van Duyne, 2006), such increases in E field enhancement of nanorattles would result in several orders of magnitude increase in SERS enhancement.

To calculate the increase in $E$ field enhancement of the nanorattle, a 3-D model of the nanorattle was built. The model was excited by an incident plane wave, and total electromagnetic field was solved. Ratio of total $E$ field and incident $E$ field, denoted $|E|/|E_{in}|$ – the E field enhancement, was calculated and plotted in Fig. 3a. Calculation results show the strong E field enhancement in the gap space of the nanorattle with the highest enhancement of about 14.10 times (Fig. 3c). This result is in agreement with previous results on a similar structure, the silica-insulated concentric structure (Lim et al., 2011). Compared to the highest E field enhancement of a gold nanosphere with similar size, which was about 3.44 times (Figs. 3b and d), the nanorattle's was 4.1 times higher. Similar improvements in $E$ field enhancement were also observed when comparing the nanorattle with the nanorattle's shell alone or with the nanorattle's core alone. The highest E field enhancement of the nanorattle's shell alone was 3.53 times (Fig. S2) while that of the nanorattle's core alone was 3.33 times (Fig. S3). However, when both the core and the shell were combined into a nanorattle with core-gap-shell structure, the highest E field enhancement was 14.10 times as mentioned above.

The strong $E$ field enhancement in the gap space of the nanorattle can be explained by the coupling of surface plasmons of the metal core and the metal shell (Xu, 2005). This strong E field enhancement between the core and the shell has been harnessed by several previous works for SERS enhancement (Chen et al., 2014; Feng et al., 2012; Gandra and Singamaneni, 2013; Jaiswal et al., 2014; Lim et al., 2011; Liu et al., 2015; Luo et al., 2011; Song et al., 2014; Xu et al., 2005; Zhou et al., 2013). Also in most of these works, only a monolayer of Raman reporters was loaded into the gap space by using self-assembly of reporters on a core followed by a shell coating. In our work, core-gap-shell structures were first synthesized followed by loading Raman reporters into the gap space. Since the gap is nanometer in scale, the nanorattle has higher reporter loading capacity.

Besides exhibiting intense SERS brightness, the core-gap-shell structure with Raman reporters trapped in the gap space between the core and the shell has several additional advantages. First, since the reporters are protected by a metal shell, chemical stability is improved with regard to signal degradation, as reporter desorption can be prevented. Similar reporter protection using silica shells has been widely reported (Doering and Nie, 2003; Kustner et al., 2009; Lee et al., 2014; Lee et al., 2012; Li et al., 2010; Liu et al., 2010; Mir-Simon et al., 2015; Sha et al., 2008). Second, since the reporters are trapped inside the structure instead of coated on the structure's outer surface, the whole outer surface is available for DNA probe functionalization. This allows more flexibility in tuning DNA probe density for optimal hybridization efficiency without compromising the SERS brightness. Third, in contrast to SERS enhancement based on nanojunctions between aggregated nanoparticles (a.k.a. SERS "hot spots") that are difficult to control and have poor reproducibility, nanorattle's SERS enhancement is based on the nanogap between the core and shell, which is easier to control and more reproducible. Due to the above merits, the nanorattle was chosen for DNA detection based on sandwich hybridization, which will be discussed in following section.

### 2.3. DNA detection

Detection of the wild type sequence of *P. falciparum* gene *PF3D7_1343700* is described in the Supplementary material using the nanorattle-based method depicted in Fig. 1. The formation of hybridization sandwiches of magnetic bead-target sequence-nanorattle was verified by SEM images (Fig. 4). In the presence of complementary target sequences, nanorattles were bound onto magnetic beads' surface (Fig. 4a). In contrast, in the absence of complementary target sequences (i.e. buffer only), almost no nanorattle was found (Fig. 4b). The result indicated that hybridization sandwiches of (1) magnetic beads loaded with capture probes, (2) target sequence, and (3) nanorattles loaded with reporter probes successfully formed in the presence of complementary target sequences. As the magnetic beads (ca. 1 μm diameter) were much bigger than the nanorattles (ca. 60 nm diameter), tens of nanorattles were found on each magnetic bead.

The quantification capability of the nanorattle-based technique was investigated by testing samples of the wild type sequence of *P. falciparum* gene *PF3D7_1343700* at different concentrations. Quantification results are shown in Fig. 5. As shown in Fig. 5a, SERS intensity decreases when target concentration decreases, suggesting that a lower number of magnetic bead-target sequence-nanorattle sandwiches were formed at lower target concentration. SERS peak intensities at 923 $cm^{-1}$ of different concentrations in Fig. 5a were normalized against the 923 $cm^{-1}$ peak intensity of the highest concentration, i.e. 100 pM, and plotted in Fig. 5b. From the results, the limit of detection was determined to be approximately 3 picomolar ($3 \times 10^{-12}$ M). Since the sample solutions' volumes were 30 μL, at 3 picomolar concentration, the copy number of target sequences was below 100 attomoles ($10^{-16}$ mol). It is noteworthy that for sample solutions at 1 nM concentration we observed detector saturation due to strong SERS signals. The linear range of our method is, therefore, expected to be between $10^{-11}$ M and $10^{-10}$ M target concentrations. For detection at higher target concentrations without detector saturation, a shorter detector's exposure time can be used.

### 2.4. SNP discrimination

SNP discrimination using SERS has been previously reported (Cao et al., 2002; Jiang et al., 2012; Johnson et al., 2012; Li et al., 2013b; Mahajan et al., 2008; Papadopoulou and Bell, 2011; Wei et al., 2013). To demonstrate the SNP discrimination capability of the nanorattle-based method, we used as models wild type and mutant DNA sequences of the malaria parasite *P. falciparum* gene *PF3D7_1343700* ("K13"). We tested 53nt K13 sequences with ("Mut") and without ("WT") a SNP encoding the C580Y substitution that confers resistance to Art-R (Ariey et al., 2014; Mohon et al., 2014). Based on the two sequences, referred to as target sequences, reporter probes for *P. falciparum* WT and of *P. falciparum* Mut were designed. A common capture probe for the two target sequences was also designed (Table S1). Samples containing *P. falciparum* WT target sequence, *P. falciparum* Mut target sequence, a non-malaria sequence, or buffer only were tested against the two reporter probes in parallel as described in the experimental section. The results are shown in Fig. 6. Both WT reporter probe and Mut reporter probe can specifically detect WT target sequence and Mut target sequence, respectively. For the WT reporter probe (Fig. 6a), the SERS intensity was high in the presence of *P. falciparum* WT target sequences. This is due to the perfect

matching between the WT reporter probes and the WT target sequences, resulting in stable double strands. More nanorattles could then attach to the magnetic beads via sandwich formation, thus resulting in high SERS intensity. However, in the presence of *P. falciparum* Mut target sequences, the SERS intensity was low (Fig. 6a). This is due to the single-base mismatch between the WT reporter probes and the Mut target sequences, resulting in less stable double strands. With the stringent washing step using low-salt washing buffer at 37 °C, these unstable double strands will dehybridize. A lower number of nanorattles were attached to the magnetic beads, resulting in low SERS intensity. For non-malaria sequence and blank, SERS intensities were close to zero (Fig. 6a), indicating that nonspecific hybridization and undesired adsorption were marginal. By dividing SERS peak intensity at 923 $cm^{-1}$ of WT probe-WT target by that of WT probe-Mut target (Fig. S5), we obtained SNP discrimination ratio of approximately 8:1 for the WT probe. Similarly, for the Mut reporter probe (Fig. 6b), SERS intensity was high in the presence of *P. falciparum* Mut target sequences and low in the presence of *P. falciparum* WT sequences. SERS intensities were close to zero for both non-malaria sequences and blank. By dividing the SERS peak intensity at 923 $cm^{-1}$ of Mut probe-Mut target by that of Mut probe-WT target (Fig. S5), the SNP discrimination ratio was determined to be approximately 3.2:1 for the Mut probe. The results clearly demonstrate the SNP discrimination capability of the nanorattle-based method.

It is noteworthy that conditions of the stringent washing step, including temperature and salt concentration, are crucial to the SNP discrimination experiment's success. To investigate the effect of temperature of the stringent washing step, we repeated the SNP discrimination experiment except that the stringent washing step was conducted at room temperature as opposed to 37 °C. The results show that the discrimination capacity was adversely affected. While the WT probe can still discriminate between WT target and Mut target but at lower discrimination ratio 2.5:1 (Fig. S6), the Mut probe couldn't discriminate between Mut target and WT target (Fig. S7). Choosing an appropriate temperature for the stringent washing step is therefore important to SNP discrimination success. Generally, this can be achieved via determining melting temperatures of perfectly-matched double strand and of single-base mismatched double strand in combination with trial-and-error. The use of two reporter probes, WT probe and Mut probe, is effective for not only SNP discrimination but also for target composition identification (Cao et al., 2002).

## 3. Conclusion

A new DNA detection method based on sandwich hybridization of magnetic bead, target sequence, and ultrabright SERS nanorattle was presented. The nanorattle has a core-gap-shell structure with Raman reporters loaded in the nanosize gap between the core and the shell. Our SERS measurements showed that the nanorattles are more than three orders of magnitude brighter than gold nanospheres loaded with the same Raman reporter. The nanorattle was used as a SERS tag for DNA detection using sandwich hybridization and magnetic beads. The current unoptimized detection limit is approximately 100 attomoles for *P. falciparum* DNA targets. SNP discrimination of wild type and mutant *P. falciparum* sequences, which confer Art-R resistance, was also demonstrated. The presented method is

simple, sensitive, and suitable for automation, making it an attractive candidate for integration into portable platforms for POC molecular diagnostics.

## Supplementary Material

Refer to Web version on PubMed Central for supplementary material.

## Acknowledgments

This work was sponsored by the National Institutes of Health (R21 AI120981-01) and the Duke Faculty Exploratory Research Fund. Hoan Thanh Ngo is supported by fellowships from the Vietnam Education Foundation and the Fitzpatrick Scholars Fellowship. S.M.T. is supported by the National Institute of Allergy and Infectious Diseases under award number K08AI100924.

## Appendix A. Supplementary material

Supplementary data associated with this article can be found in the online version at http://dx.doi.org/10.1016/j.bios.2016.01.073.

## References

Ariey F, Witkowski B, Amaratunga C, Beghain J, Langlois AC, Khim N, Kim S, Duru V, Bouchier C, Ma L, Lim P, Leang R, Duong S, Sreng S, Suon S, Chuor CM, Bout DM, Menard S, Rogers WO, Genton B, Fandeur T, Miotto O, Ringwald P, Le Bras J, Berry A, Barale JC, Fairhurst RM, Benoit-Vical F, Mercereau-Puijalon O, Menard D. Nature. 2014; 505(7481):50–55. [PubMed: 24352242]

Bessetti J. Profiles in DNA. 2007; 10(1):9–10.

Cao YWC, Jin RC, Mirkin CA. Science. 2002; 297(5586):1536–1540. [PubMed: 12202825]

Chen HM, Liu RS, Asakura K, Lee JF, Jang LY, Hu SF. J Phys Chem B. 2006; 110(39):19162–19167. [PubMed: 17004764]

Chen Z, Yu D, Huang Y, Zhang Z, Liu T, Zhan J. Sci Rep. 2014; 4:6709. [PubMed: 25335862]

Darby BL, Etchegoin PG, Le Ru EC. Phys Chem Chem Phys. 2014; 16(43):23895–23899. [PubMed: 25277821]

Doering WE, Nie S. Anal Chem. 2003; 75(22):6171–6176. [PubMed: 14615997]

Dondorp AM, Nosten F, Yi P, Das D, Phyo AP, Tarning J, Lwin KM, Ariey F, Hanpithakong W, Lee SJ, Ringwald P, Silamut K, Imwong M, Chotivanich K, Lim P, Herdman T, An SS, Yeung S, Singhasivanon P, Day NPJ, Lin-degardh N, Socheat D, White NJ. New Engl J Med. 2009; 361(17): 1714.

Donnelly T, Smith WE, Faulds K, Graham D. Chem Commun. 2014; 50(85):12907–12910.

Fabris L, Dante M, Braun G, Lee SJ, Reich NO, Moskovits M, Nguyen TQ, Bazan GC. J Am Chem Soc. 2007; 129(19):6086–6087. [PubMed: 17451246]

Faulds K, Barbagallo RP, Keer JT, Smith WE, Graham D. Analyst. 2004; 129(7):567–568. [PubMed: 15213819]

Faulds K, Jarvis R, Smith WE, Graham D, Goodacre R. Analyst. 2008; 133(11):1505–1512. [PubMed: 18936827]

Feng YH, Wang Y, Wang H, Chen T, Tay YY, Yao L, Yan QY, Li SZ, Chen HY. Small. 2012; 8(2): 246–251. [PubMed: 22125121]

Gandra N, Singamaneni S. Adv Mater. 2013; 25(7):1022–1027. [PubMed: 23161698]

Gao FL, Lei JP, Ju HX. Anal Chem. 2013; 85(24):11788–11793. [PubMed: 24171654]

He Y, Su S, Xu TT, Zhong YL, Zapien JA, Li J, Fan CH, Lee ST. Nano Today. 2011; 6(2):122–130.

Hu J, Zheng PC, Jiang JH, Shen GL, Yu RQ, Liu GK. Analyst. 2010; 135(5):1084–1089. [PubMed: 20419260]

Jaiswal A, Tian LM, Tadepalli S, Liu KK, Fei M, Farrell ME, Pellegrino PM, Singamaneni S. Small. 2014; 10(21):4287–4292. [PubMed: 25045064]

Jiang ZY, Jiang XX, Su S, Wei XP, Lee ST, He Y. Appl Phys Lett. 2012; 100(20)

Johnson RP, Richardson JA, Brown T, Bartlett PN. J Am Chem Soc. 2012; 134(34):14099–14107. [PubMed: 22835041]

Kang T, Yoo SM, Yoon I, Lee SY, Kim B. Nano Lett. 2010; 10(4):1189–1193. [PubMed: 20222740]

Khalavka Y, Becker J, Sonnichsen C. J Am Chem Soc. 2009; 131(5):1871–1875. [PubMed: 19154114]

Kneipp K, Wang Y, Kneipp H, Perelman LT, Itzkan I, Dasari R, Feld MS. Phys Rev Lett. 1997; 78(9): 1667–1670.

Kustner B, Gellner M, Schutz M, Schoppler F, Marx A, Strobel P, Adam P, Schmuck C, Schlucker S. Angew Chem Int Ed. 2009; 48(11):1950–1953.

Lane LA, Qian XM, Nie SM. Chem Rev. 2015; 115(19):10489–10529. [PubMed: 26313254]

Lee S, Chon H, Yoon SY, Lee EK, Chang SI, Lim DW, Choo J. Nanoscale. 2012; 4(1):124–129. [PubMed: 22080302]

Lee S, Chon H, Lee J, Ko J, Chung BH, Lim DW, Choo J. Biosens Bioelectron. 2014; 51:238–243. [PubMed: 23973735]

Li JF, Huang YF, Ding Y, Yang ZL, Li SB, Zhou XS, Fan FR, Zhang W, Zhou ZY, WuDe Y, Ren B, Wang ZL, Tian ZQ. Nature. 2010; 464(7287):392–395. [PubMed: 20237566]

Li JM, Ma WF, You LJ, Guo J, Hu J, Wang CC. Langmuir. 2013a; 29(20):6147–6155. [PubMed: 23611465]

Li JM, Wei C, Ma WF, An Q, Guo J, Hu J, Wang CC. J Mater Chem. 2012; 22(24):12100–12106.

Li M, Cushing SK, Liang HY, Suri S, Ma DL, Wu NQ. Anal Chem. 2013b; 85(4):2072–2078. [PubMed: 23320458]

Lim DK, Jeon KS, Hwang JH, Kim H, Kwon S, Suh YD, Nam JM. Nat Nanotechnol. 2011; 6(7):452–460. [PubMed: 21623360]

Liu KK, Tadepalli S, Tian L, Singamaneni S. Chem Mater. 2015; 27(15):5261–5270.

Liu X, Knauer M, Ivleva NP, Niessner R, Haisch C. Anal Chem. 2010; 82(1):441–446. [PubMed: 19957963]

Luo Z, Chen K, Lu D, Han H, Zou M. Microchim Acta. 2011; 173(1–2):149–156.

Mahajan S, Richardson J, Brown T, Bartlett PN. J Am Chem Soc. 2008; 130(46):15589–15601. [PubMed: 19006412]

Mayr R, Haider M, Thünauer R, Haselgrübler T, Schütz GJ, Sonnleitner A, Hesse J. Biosens Bioelectron. 2016; 78:1–6. [PubMed: 26580983]

Mir-Simon B, Reche-Perez I, Guerrini L, Pazos-Perez N, Alvarez-Puebla RA. Chem Mater. 2015; 27(3):950–958.

Mohon A, Alam MS, Bayih AG, Folefoc A, Shahinas D, Haque R, Pillai DR. Malaria J. 2014; 13

Moon GD, Choi SW, Cai X, Li WY, Cho EC, Jeong U, Wang LV, Xia YN. J Am Chem Soc. 2011; 133(13):4762–4765. [PubMed: 21401092]

Ngo H, Wang HN, Burke T, Ginsburg G, Vo-Dinh T. Anal Bioanal Chem. 2014a; 406(14):3335–3344. [PubMed: 24577572]

Ngo HT, Wang HN, Fales AM, Vo-Dinh T. Anal Chem. 2013; 85(13):6378–6383. [PubMed: 23718777]

Ngo HT, Wang HN, Fales AM, Vo-Dinh T. Anal Bioanal Chem. 2015:1–9.

Ngo HT, Wang HN, Fales AM, Nicholson BP, Woods CW, Vo-Dinh T. Analyst. 2014b; 139(22):5655–5659. [PubMed: 25248522]

Nie SM, Emery SR. Science. 1997; 275(5303):1102–1106. [PubMed: 9027306]

Niemz A, Ferguson TM, Boyle DS. Trends Biotechnol. 2011; 29(5):240–250. [PubMed: 21377748]

Noedl H, Se Y, Schaecher K, Smith BL, Socheat D, Fukuda MM, Consortium A.S. New Engl J Med. 2008; 359(24):2619–2620. [PubMed: 19064625]

Papadopoulou E, Bell SEJ. Angew Chem Int Edit. 2011; 50(39):9058–9061.

Qi J, Zeng J, Zhao F, Lin SH, Raja B, Strych U, Willson RC, Shih WC. Nanoscale. 2014; 6(15):8521–8526. [PubMed: 24953169]

Schatz, GC.; Van Duyne, RP. Electromagnetic Mechanism of Surface-Enhanced Spectroscopy Handbook of Vibrational Spectroscopy. John Wiley & Sons, Ltd; New York: 2006.

Schlücker S. Angew Chem Int Edit. 2014; 53(19):4756–4795.

Sha MY, Xu H, Natan MJ, Cromer R. J Am Chem Soc. 2008; 130(51):17214–17215. [PubMed: 19053187]

Song J, Duan B, Wang C, Zhou J, Pu L, Fang Z, Wang P, Lim TT, Duan H. J Am Chem Soc. 2014; 136(19):6838–6841. [PubMed: 24773367]

Sun L, Yu CX, Irudayaraj J. Anal Chem. 2007; 79(11):3981–3988. [PubMed: 17465531]

Sun YG, Wiley B, Li ZY, Xia YN. J Am Chem Soc. 2004; 126(30):9399–9406. [PubMed: 15281832]

Vo-Dinh T. Trac-Trend Anal Chem. 1998; 17(8–9):557–582.

Vo-Dinh T, Dhawan A, Norton SJ, Khoury CG, Wang HN, Misra V, Gerhold MD. J Phys Chem C. 2010; 114(16):7480–7488.

Vo-Dinh T, Liu Y, Fales AM, Ngo H, Wang HN, Register JK, Yuan H, Norton SJ, Griffin GD. WIRES Nanomed Nanobiotechnol. 2015; 7(1):17–33.

Vo-Dinh T, Fales AM, Griffin GD, Khoury CG, Liu Y, Ngo H, Norton SJ, Register JK, Wang HN, Yuan H. Nanoscale. 2013; 5(21):10127–10140. [PubMed: 24056945]

Wei XP, Su S, Guo YY, Jiang XX, Zhong YL, Su YY, Fan CH, Lee ST, He Y. Small. 2013; 9(15): 2493–2499. [PubMed: 23359560]

WHO. World Malaria Report 2013. World Health Organization; Geneva: 2014.

Xia XH, Wang Y, Ruditskiy A, Xia YN. Adv Mater. 2013; 25(44):6313–6333. [PubMed: 24027074]

Xu, H.; Sha, M.; Cromer, R.; Penn, S.; Holland, E.; Chakarova, G.; Natan, M. Portable SERS sensor for sensitive detection of food-borne pathogens. In: Ku-mar, CSR., editor. Raman Spectroscopy for Nanomaterials Characterization. Springer; Berlin, Heidelberg: 2012. p. 531-551.

Xu HX. Phys Rev B. 2005; 72(7)

Xu LJ, Lei ZC, Li JX, Zong C, Yang CJ, Ren B. J Am Chem Soc. 2015; 137(15):5149–5154. [PubMed: 25835155]

Xu S, Zhao B, Xu W, Fan Y. Colloid Surf A. 2005:257–258.

Zhang H, Harpster MH, Park HJ, Johnson PA. Anal Chem. 2011; 83(1):254–260. [PubMed: 21121693]

Zhou Y, Lee C, Zhang J, Zhang P. J Mater Chem C. 2013; 1(23):3695–3699.

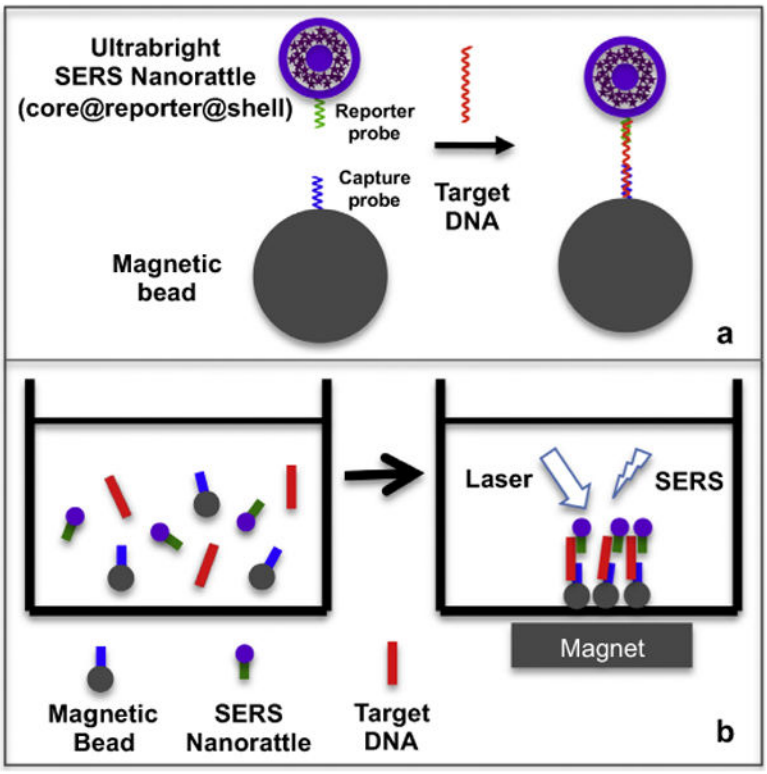


**Fig. 1.**

(a) The nanorattle-based DNA detection method using sandwich hybridization of (1) magnetic bead that are loaded with capture probes, (2) target sequence, and (3) ultrabright SERS nanorattles that are loaded with reporter probes. (b) A magnet is applied to concentrate the hybridization sandwiches at a detection spot for SERS measurements.

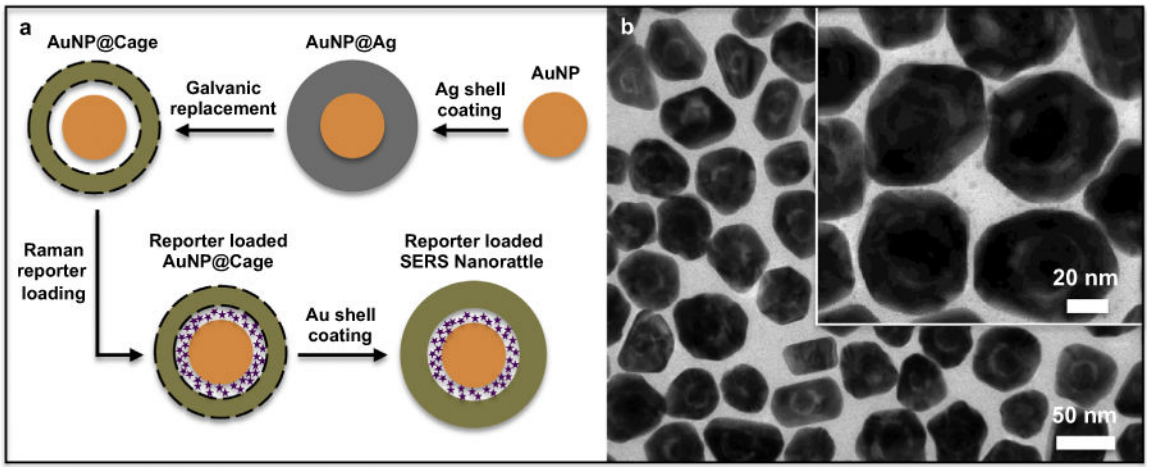


**Fig. 2.**

(a) SERS nanorattle synthesis process. (b) TEM image of nanorattles with core-gap-shell structure (inset: higher magnification TEM image). Raman reporters were loaded into the gap space between the core and the shell.

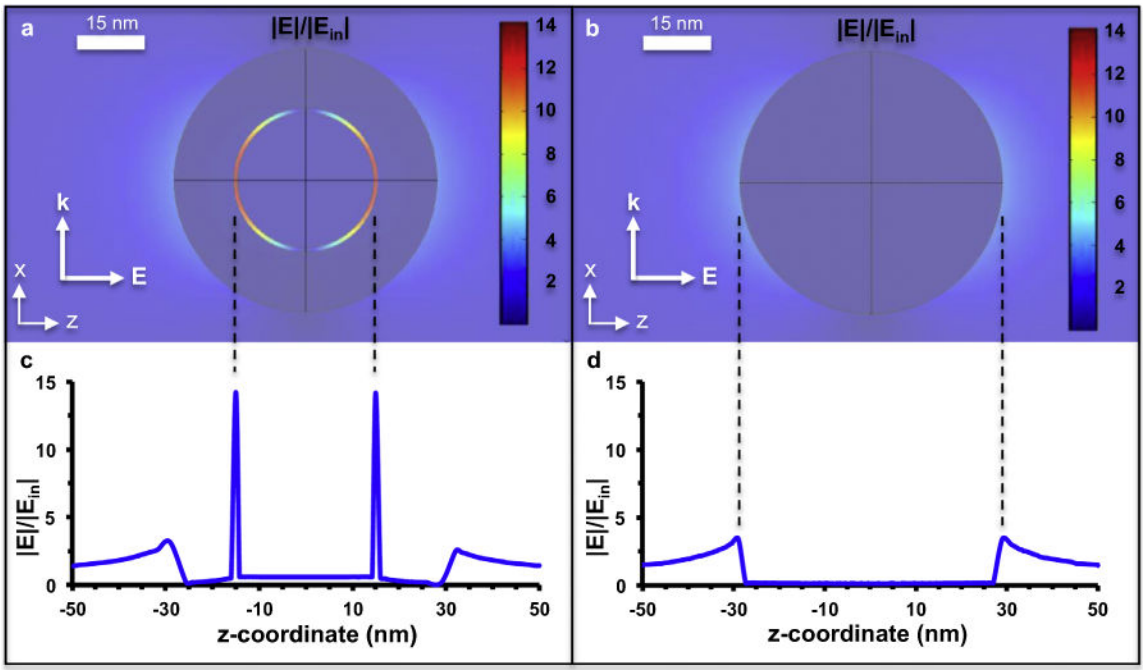


**Fig. 3.**

*E* field enhancement of nanorattle (a) and nanosphere (b). High *E* field enhancement in the gap space between nanorattle's core and shell can be observed. E field enhancement along *z*-axis crossing though nanorattle's center (c) and nanosphere's center (d).

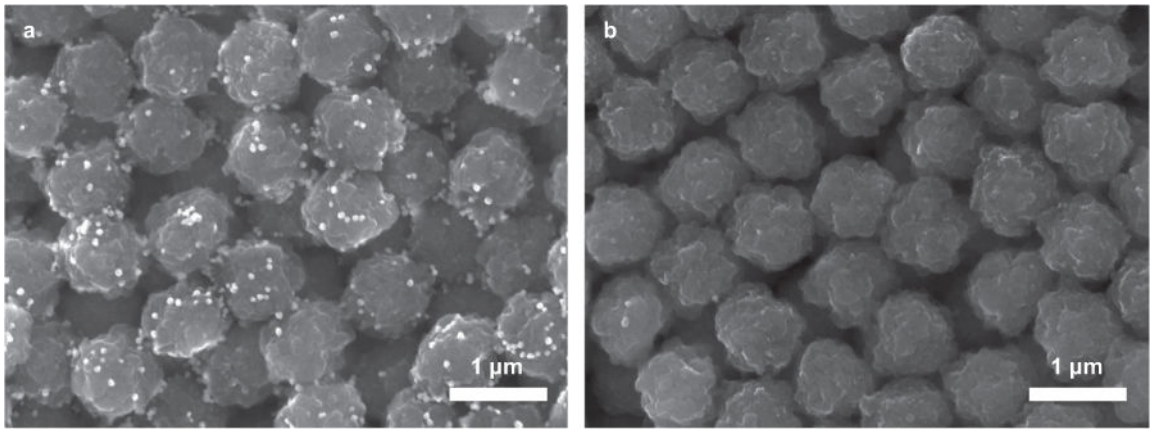


**Fig. 4.**

(a) SEM image of nanorattles bound onto magnetic beads' surface in the presence of complementary target sequences. (b) Almost no nanorattle found on magnetic beads in the absence of complementary target sequences.

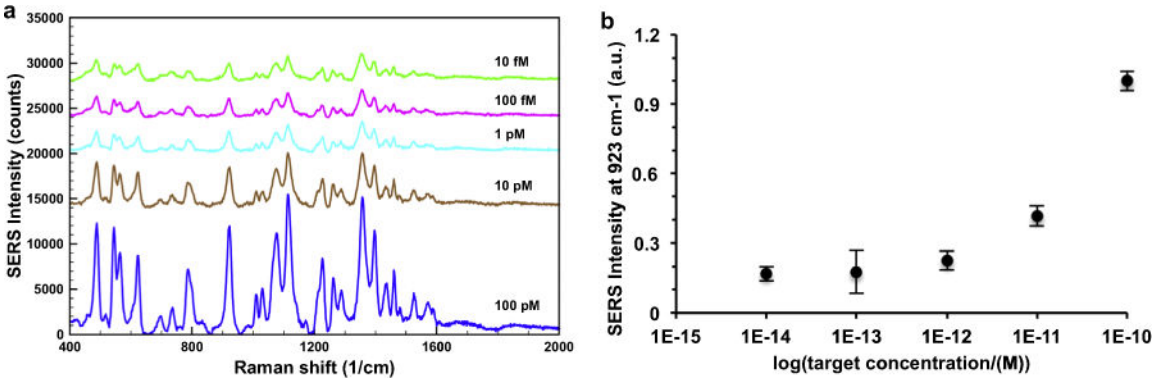


**Fig. 5.**

(a) SERS spectra at different concentrations of wild type target *P. falciparum* gene *PF3D7_1343700* (vertically shifted for clarity). (b) SERS intensities at 923 $cm^{-1}$ (normalized) vs. log(target concentration/(M)). Error bars represent standard deviations ($n$ = 3).

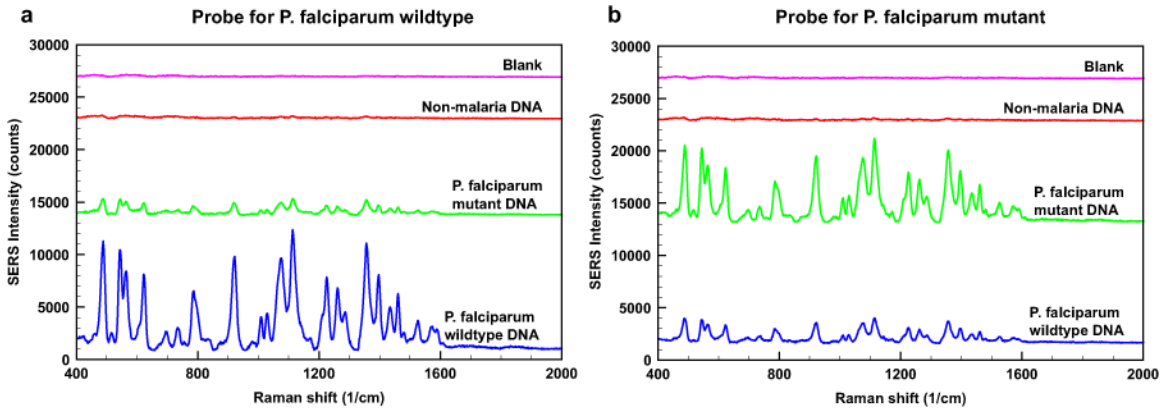


**Fig. 6.**

Detection of wild type *P. falciparum* and mutant *P. falciparum* with a single nucleotide difference using the nanorattle-based method (vertically shifted for clarity). Two probes, one for wild type *P. falciparum* (a) and one for mutant *P. falciparum* (b), were designed and tested against *P. falciparum* wild type DNA, *P. falciparum* mutant DNA, non-malaria DNA, and blank. The wild type DNA and the mutant DNA have a single base difference.